

Understanding Recent Stratospheric Climate Change

David W. J. Thompson
Department of Atmospheric Science
Colorado State University
Fort Collins, CO.

Susan Solomon
Chemical Sciences Division
Earth System Research Laboratory
National Oceanic and Atmospheric Administration
Boulder, CO.

Submitted to the Journal of Climate
February 2008

Revised
July 2008, October 2008

Accepted
October 2008

Abstract

The long-term, global-mean cooling of the lower stratosphere stems from two downward steps in temperature, both of which are coincident with the cessation of transient warming after the volcanic eruptions of El Chichon and Mt. Pinatubo. Previous attribution studies reveal that the long-term cooling is linked to ozone trends, and modeling studies driven by a range of known forcings suggest that the steps reflect the superposition of the cooling with transient variability in upwelling longwave radiation from the troposphere. However, the long-term cooling of the lower stratosphere is evident at all latitudes despite the fact that chemical ozone losses are thought to be greatest at middle and polar latitudes. Further, the ozone concentrations used in such studies are based on either *a*) smooth mathematical functions fit to sparsely sampled observations that are unavailable during post-volcanic periods or *b*) calculations by a coupled chemistry-climate model.

Here we provide observational analyses that yield new insight into three key aspects of recent stratospheric climate change. First, we provide evidence that the unusual step-like behavior of global-mean stratospheric temperatures is dependent not only upon the trend but also on the temporal variability in global-mean ozone immediately following volcanic eruptions. Second, we argue that the warming/cooling pattern in global-mean temperatures following major volcanic eruptions is consistent with the competing radiative and chemical effects of volcanic eruptions on stratospheric temperature and ozone. Third, we reveal the contrasting latitudinal structures of recent stratospheric temperature and ozone trends are consistent with large-scale increases in the stratospheric overturning Brewer-Dobson circulation.

1. Introduction

The lower stratosphere has cooled by a globally averaged $\sim 0.3\text{-}0.5$ K/decade since 1979 (Ramaswamy et al. 2001; WMO 2007, Chapter 5; Randel et al. 2008). The global-mean cooling has not occurred monotonically, but rather is manifested as two downward “steps” in temperature, both of which are coincident with the cessation of transient warming after the major volcanic eruptions of El Chichon and Mt. Pinatubo (Pawson et al. 1998; Seidel and Lanzante 2004; Ramaswamy et al. 2006). The lower stratosphere has not noticeably cooled since 1995, which indicates that the trends in this region are not dominantly controlled by the known increases in carbon dioxide over this period (Ramaswamy et al. 2006).

Attribution experiments indicate that the long-term cooling in global-mean lower stratospheric temperatures is driven mainly by changes in stratospheric ozone (e.g., Rosier and Shine 2000; Ramaswamy and Schwarzkopf 2002; Shine et al. 2003; Langematz et al. 2003; Ramaswamy et al. 2006). Ramaswamy et al. (2006) argue that the step-like behavior in global-mean stratospheric temperatures is due primarily to the juxtaposition of the long-term cooling on variability in upwelling longwave radiation from the troposphere. Dameris et al. (2005) and Ramaswamy et al. (2006) both theorize that the solar cycle may also have contributed to the flattening of the temperature trends after recent major volcanic eruptions.

The stratospheric ozone concentrations used in previous attribution experiments are based on either *a*) sparsely sampled profile measurements fitted to a predetermined number of physical factors (e.g., the Randel and Wu 2007 dataset) or *b*) simulated values from coupled chemistry-climate models (CCMs). The uncertainties inherent in the ozone

data used in such experiments have important implications for understanding the relationships between stratospheric ozone and temperatures, particularly during the period immediately following both volcanic eruptions. For example, the Randel and Wu (2007) dataset is not expected to capture the full variability in ozone following volcanic eruptions for two reasons: 1) the dataset is based on fits to time series of the Quasi-Biennial Oscillation, the solar cycle, and decadal trends, but does not include a volcanic term in the regression; and 2) the dataset is based on the Stratospheric Aerosol and Gas Experiment (SAGE) data equatorward of 60 degrees, but the SAGE data are unreliable during the two year period following volcanic eruptions (Wang et al 2002). The predicted values of ozone following volcanic eruptions vary substantially from one CCM simulation to the next (Eyring et al. 2006).

The spatial structures of recent stratospheric temperature and ozone trends have proven difficult to reconcile with each other. Stratospheric temperatures are decreasing at a comparable rate at all latitudes (Thompson and Solomon 2005; Randel et al. 2008), but ozone is generally thought to be decreasing most at middle and polar latitudes (Chipperfield et al. 2007). The tropical stratospheric cooling is robust (Thompson and Solomon 2005; Randel et al. 2008), albeit the amplitude of the trends at select radiosonde stations may be impacted by changes in instrumentation (Randel and Wu 2006). In contrast, the tropical ozone trends remain unclear: profile data from the SAGE instrument suggest ozone levels are decreasing in the lower tropical stratosphere (Chipperfield et al. 2007; Forster et al. 2007; Randel and Wu 2007), but the SAGE data have sparse temporal and spatial coverage, and similar trends are not reflected in total column ozone data (Chipperfield et al. 2007; Randel and Wu 2007). The tropical SAGE trends are consistent

with the tropical column trends if tropical tropospheric ozone is assumed to have increased by ~15%, but trends in tropical tropospheric ozone are highly uncertain and vary substantially from dataset to dataset (Chipperfield et al. 2007). As such, the differences between tropical column and profile measurements may be real, but the differences are smaller than the uncertainties in the measurements.

The uncertainty in tropical ozone trends is important since the attribution of lower stratospheric temperature trends depends on the ozone trend dataset used in the analyses. For example, in the Randel and Wu (1999) dataset, tropical lower stratospheric ozone trends are pinned to the column trends, whereas in the Randel and Wu (2007) dataset, tropical lower stratospheric ozone trends are derived from the SAGE II data. Since the tropical SAGE II and column trends differ considerably (Chipperfield et al. 2007; Randel and Wu 2007), attribution studies based on the 1999 dataset yield largest cooling at middle and polar latitudes (c.f. Fig. 7 from Shine et al. 2003), whereas attribution studies based on the 2007 study yield comparable cooling at all latitudes (e.g., Ramaswamy 2006). Several recent climate change experiments exhibit cooling in the tropical stratosphere not from decreases in ozone there, but from increases in the model stratospheric overturning circulation (e.g., Rind et al. 1998; Butchart and Scaife 2001; Eichelberger and Hartmann 2005; Li et al. 2008). The implications of our results for those studies is discussed in the conclusions.

Here we exploit the excellent space/time coverage afforded by total column ozone and the relationships between column ozone and stratospheric temperatures to gain new insights into recent stratospheric climate change. We provide new evidence that the step-like behavior in global-mean stratospheric temperatures does not depend on various

physical factors as argued in previous studies, but rather is linearly congruent with the temporal variability in ozone following volcanic eruptions. We offer new analyses that suggest the warming/cooling pattern seen in association with the eruptions of El Chichon and Mt. Pinatubo is consistent with the competing radiative and chemical effects of these geophysical events. Finally, we exploit a fitting procedure that reveals the contrasting horizontal structures of stratospheric ozone and temperature trends are consistent with increases in the stratospheric overturning Brewer-Dobson circulation.

In section 2 we discuss the data used in the study; in section 3 we examine the relationships between the time history of global-mean ozone and stratospheric temperatures; and in section 4 we provide insights into the horizontal structure of stratospheric temperature trends. Concluding remarks are given in Section 5.

2. Data and analysis details

The primary data used in the analyses are monthly-mean temperature retrievals from the Microwave Sounding Unit Channel 4 (MSU4) and total column ozone measurements from the merged Total Ozone Mapping Spectrometer/Solar Backscatter Ultraviolet dataset (TOMS/SBUV).

The MSU4 data are indicative of temperatures averaged over a broad layer of the atmosphere extending from ~250-30 hPa with peak amplitude near ~90 hPa. The majority of the MSU4 weighting function lies in the lower stratosphere, but a small component also resides in the upper troposphere, particularly in the tropics where the tropopause reaches ~100 hPa (Fig. 1a). The MSU4 data are provided by Remote Sensing Systems

and sponsored by the NOAA Climate and Global Change Program (Mears et al. 2003; <http://www.remss.com>).

The merged TOMS/SBUV data are constructed by the TOMS science team at the National Aeronautics and Space Administration Goddard Space Flight Center and are available via <http://code916.gsfc.nasa.gov> (Stolarski et al. 2006). The reproducibility of select results based on the TOMS/SBUV data is assessed using global-wide ground based total column measurements provided courtesy of V. Fioletov at Environment Canada (Fioletov et al. 2002).

We also make brief use of monthly-mean Stratospheric Aerosol and Gas Experiment (SAGE) II measurements (McCormick et al. 1989), which are available November 1984-August 2005. The SAGE II results shown here are presented in units of Dobson Units per kilometer (DU/km).

The seasonal cycle is removed from the monthly-mean data to form anomalies by subtracting the long-term monthly-means from the data as a function of calendar month. Linear trends are calculated for the period 1979-2006. Trend, regression and correlation coefficients based on the MSU4 temperature data are based on all months 1979-2006 except for the three year periods following the eruptions of El Chichon and Mt. Pinatubo to minimize the impact of the large transient warming following both eruptions. The significance of the trend calculations is estimated using the methodology outlined in Santer et al. (2000), and the significance of the correlations is assessed using the t -statistic based on the appropriate number of degrees of freedom.

3. The signature of ozone in the time history of global-mean stratospheric temperatures

On regional scales, ozone and stratospheric temperatures are linked via the absorption of shortwave radiation by ozone, the absorption and emission of longwave radiation by ozone, and by virtue of the fact that both ozone and temperatures are impacted by variability in the atmospheric flow. In the global-mean, the effect of atmospheric motions on stratospheric temperatures and ozone largely cancel (Yulaeva et al. 1994), and hence the relationship between stratospheric temperatures and ozone reduces to the radiative impacts of ozone.

It is difficult to assess the relationships between global-mean stratospheric ozone and temperature within a narrow vertical region of the atmosphere using observations alone because of the poor spatial and temporal sampling afforded by ozone profile data. In-situ ozonesonde measurements are available at only a handful of stations extending back to the 1980s; the remotely-sensed SAGE profile data have numerous spatial and temporal gaps and are not reliable during periods of high stratospheric loadings of volcanic aerosols (Wang et al 2002). The sparse nature of ozone profile data is why datasets used in attribution studies are provided as linear fits to a select number of physical forcings and do not capture the full variability in ozone following volcanic eruptions (e.g., the Randel and Wu 2007 dataset used in Ramaswamy et al. 2006).

In contrast to profile ozone measurements, total column measurements from the TOMS/SBUV data have excellent temporal and spatial sampling, and relatively small estimated aerosol-contamination errors during periods immediately following volcanic

eruptions (e.g., Bhartia et al. 1993). At first glance, the TOMS/SBUV data appear ill-suited for examining the relationships between stratospheric ozone and temperatures since column measurements sample the entire atmosphere. However, in practice, there is substantial overlap between the MSU4 weighting function and the region of the atmosphere that contributes most to variations in globally averaged column ozone (e.g., Randel and Cobb 1994). For example, the solid line in Fig. 1a shows the weighting function for the MSU4 instrument, and the dashed line in Fig. 1a shows the regression of the monthly-mean, global-mean anomaly time series from the SAGE II data as a function of altitude onto the monthly-mean, global-mean anomaly time series of column ozone from the TOMS/SBUV data. Both the solid and dashed lines are normalized such that the area under the curves is equal to one. As evidenced in Fig. 1a, most of the variability in column ozone derives from variations in the lower stratosphere. The considerable overlap between the dashed and solid lines in Fig. 1a suggests that variability in global-mean column ozone can be used as a proxy for variability in ozone within the region sampled by the MSU4 instrument.

Figures 1b and 1c show the scatter plot and time series, respectively, for global-mean MSU4 temperatures (T_4) and column ozone from the TOMS/SBUV data (O_3). With the exception of the two brief periods of volcanically induced warming, the two time series exhibit a remarkable degree of covariability. Many of the high frequency excursions in global-mean T_4 are mirrored in global-mean O_3 , and both time series exhibit drops between ~1982-4, slight increases between ~1984-1991, drops again between ~1991-3, and weak rises between ~1993 and the present.

The contribution of variability in global-mean O_3 to global-mean T_4 can be

quantified by decomposing the data into components linearly congruent with and linearly independent of variations in column ozone as follows:

$$(1) \quad \langle T_4^{O_3}(t) \rangle = \frac{\overline{\langle O_3(t) \rangle \langle T_4(t) \rangle}}{\langle O_3(t) \rangle^2} \cdot \langle O_3(t) \rangle$$

where $\langle \rangle$ denotes the global-mean, the overbar denotes the time-mean; $\langle O_3(t) \rangle$ corresponds to the global-mean total column ozone anomaly time series (in units of DU); the fractional term on the right hand side corresponds to the regression of $\langle T_4(t) \rangle$ onto $\langle O_3(t) \rangle$, calculated for periods with low volcanic forcing (in units K/DU; see Section 2 for the definition of periods of low volcanic forcing); and $\langle T_4^{O_3}(t) \rangle$ denotes the component of $\langle T_4(t) \rangle$ that is linearly congruent with variations in $\langle O_3(t) \rangle$ (in units K).

The ozone-residual global-mean temperature time series ($\langle T_4^*(t) \rangle$) is found by subtracting $\langle T_4^{O_3}(t) \rangle$ from $\langle T_4(t) \rangle$. By construction, $\langle T_4^*(t) \rangle$ corresponds to the component of $\langle T_4(t) \rangle$ that is linearly unrelated to fluctuations in $\langle O_3(t) \rangle$ during periods of low volcanic forcing.

The results of the fitting procedure (Figure 2) highlight three aspects of global-mean stratospheric temperature variability:

1) The drops in lower stratospheric temperatures following the eruptions of El-Chichon and Mt. Pinatubo are linearly consistent with the temporal behavior of global-mean ozone during the ~ 2 years following both eruptions. When the linear relationship

with ozone is regressed from the data, stratospheric temperatures recover to pre-eruption values by ~1984 and ~1994.

2) The weak rise of temperatures between ~1984 and ~1991 is consistent with the weak rise in global-mean ozone depletion at this time.

3) The warming of the stratosphere since the eruption of Mt. Pinatubo is largely driven by the recent increases in global-mean ozone. In fact, when the linear relationship with ozone is regressed from the data, stratospheric temperatures have decreased since the eruption of Mt. Pinatubo. The decreases in the residual temperature data since the mid 1990s can be interpreted as reflecting physical processes other than ozone depletion, and are broadly consistent with the predicted impact of increasing greenhouse gases (Shine et al. 2003; Ramaswamy et al. 2006).

Why did global-mean column ozone drop during the periods immediately following the eruptions of El Chichon and Mt. Pinatubo (Fig. 2; Gleason et al. 1993; Chipperfield et al. 2007)? Volcanic eruptions are known to have two primary impacts on stratospheric composition: increased sulfate aerosol loading and decreased concentrations of stratospheric ozone (e.g., Solomon et al. 1996; Robock 2000). The heating effect of the aerosols depends linearly on the aerosol mass and is only evident for a year or two after the eruption date. In contrast, the chemical effects and resulting depletion of ozone require the presence of chlorine, depend on highly nonlinear nitrogen oxide and chlorine oxide chemistry, and saturate for relatively small aerosol loadings (Prather 1992; Solomon et al. 1996). The nonlinearity of the chemical effect on ozone is important, as it means the cooling effect of volcanoes can 1) remain substantial as the direct warming effect diminishes and 2) persist for several years after the aerosol loading has declined

from its largest values.

Previous analyses have questioned whether the eruption of Mt. Pinatubo had a global effect on ozone, and the apparent lack of SH midlatitude column ozone losses following the Mt. Pinatubo eruption is highlighted as an outstanding research question in the 2006 Ozone Assessment (Chipperfield et al. 2007). However, when the anomalies in TOMS/SBUV data are viewed as a function of latitude and time, drops in ozone appear to occur across much of the globe during the five-year period following the Mt. Pinatubo eruption date (Fig. 3a; recall the seasonal cycle is removed from all data in the paper). Short-term temporal variability obscures the signal at particular latitudes and in certain seasons, and the Quasi-Biennial Oscillation has a strong effect, including at southern mid-latitudes (Bodecker et al. 2007; Fleming et al., 2007). Further, the SH polar region exhibits strong ozone depletion long after the period of volcanic forcing. Nevertheless, it is apparent from both the time/latitude plot in Fig. 3a and the time series in Fig. 4 that the several-year period after the eruption of Mt. Pinatubo is unique in the global ozone record, insofar as it is the only period in which concurrent ozone decreases are observed across not only the tropics and NH midlatitudes, but also SH midlatitudes.

4. Interpretation of the meridional structures associated with recent ozone and stratospheric temperature trends

The stratosphere is cooling at all latitudes, but the cooling is most significant at tropical latitudes and is obscured by a string of relatively warm years since 2000 at polar latitudes (Fig. 3b; Fig. 5 middle; Fig. 6 see also Thompson and Solomon 2005). In

contrast, column ozone has decreased markedly in the polar regions (especially in the SH) but has not dropped notably in the tropics (Fig. 3a; Fig. 5 bottom; Fig. 6; see also Chipperfield et al. 2007). In this section we extend the fitting procedure used in Section 3 to provide our own interpretation of the different meridional structures associated with recent ozone and stratospheric temperature trends.

Zonal-mean temperatures are divided into components linearly congruent with and linearly independent of variations in ozone as follows:

$$(2) \quad T_4^{O_3}(\theta, t) = \frac{\overline{O_3(\theta, t) \cdot T_4(\theta, t)}}{O_3(\theta, t)^2} \cdot O_3(\theta, t)$$

where $O_3(\theta, t)$ corresponds to the total column ozone anomaly time series as a function of latitude band θ (the latitude bands are 5 degrees in width); the overbar denotes the time-mean; the fractional term on the right-hand side corresponds to the regression of $T_4(\theta, t)$ onto $O_3(\theta, t)$ as a function of latitude, calculated as in Eq. 1 for periods with no volcanic forcing; and $T_4^{O_3}(\theta, t)$ denotes the component of $T_4(\theta, t)$ linearly congruent with variations in $O_3(\theta, t)$. The corresponding ozone-residual temperature time series $T_4^*(\theta, t)$ are found for all latitude bands as $T_4(\theta, t) - T_4^{O_3}(\theta, t)$. As in Eq. 1, along a given latitude band $T_4^*(\theta, t)$ denotes the component of $T_4(\theta, t)$ that is linearly uncorrelated to fluctuations in $O_3(\theta, t)$ during periods of low volcanic forcing. The trends in stratospheric temperatures linearly congruent with and linearly unrelated to changes in total column

ozone are found by calculating the linear trends in $T_4^{O_3}(\theta, t)$ and $T_4^*(\theta, t)$, respectively.

The fitting procedure in (2) does not relate temperature and ozone variability to specific physical phenomena as done in, for example, Randel and Cobb (1994) and Steinbrecht et al. (2003). Rather it isolates the component of the variance in the temperature field that is linearly related to variability in column ozone. In contrast to the case of the global-mean, the fitted temperature time series $T_4^{O_3}(\theta, t)$ reflect the effect of not only radiative processes but also dynamic variability. Radiative processes contribute to the regression coefficients in (2) for periods longer than the ~one-two month radiative timescale in the lower stratosphere; dynamic variability contributes to the regression coefficients on both month-to-month and longer timescales (e.g., Randel and Cobb 1994).

The overlapping influence of dynamics and radiative processes in the fitting procedure in (2) can be interpreted in the context of the following simplification of the zonal-mean thermodynamic energy equation:

$$(3) \quad \frac{\partial}{\partial t} T_4 \approx S\omega^{O_3} + S\omega^* + Q^{O_3^{dyn}} + Q^{O_3^{chem}} + other$$

where T_4 denotes MSU4 temperatures, $Q^{O_3^{dyn}}$ and $Q^{O_3^{chem}}$ correspond to radiative forcing by the components of the ozone distribution determined by dynamical and chemical processes, respectively, and $S\omega^{O_3}$ and $S\omega^*$ correspond to adiabatic temperature changes by the components of the atmospheric flow linearly congruent with and linearly unrelated to the distribution of ozone, respectively (S denotes static stability and ω vertical

velocity). By construction, the terms $Q^{O_3^{dyn}}$ and $S\omega^{O_3}$ are perfectly correlated but have amplitudes determined by their respective physical processes (e.g., radiative transfer and compressional warming/expansional cooling).

Ideally, the fitting procedure in (2) would isolate the radiative effects of ozone ($Q^{O_3^{dyn}} + Q^{O_3^{chem}}$) from adiabatic temperature changes ($S\omega^{O_3} + S\omega^*$). However, on regional scales dynamics impact both temperature advection and the distribution of ozone, so that the fitting procedure instead isolates the term $S\omega^{O_3} + Q^{O_3^{dyn}} + Q^{O_3^{chem}}$ from the term $S\omega^*$. That is to say: the residual temperature time series in (2) reflect temperature advection only by the component of the atmospheric flow that is linearly uncorrelated with variability in ozone.

The residual time series in (2) may be expected to underestimate the impact of atmospheric dynamics on atmospheric temperatures in regions of rising and sinking motion. For example: in regions of anomalous subsidence, ozone is increased via dynamical processes, and temperatures increase due to both compressional warming and the radiative effects of the additional ozone. Since the terms $S\omega^{O_3}$ and $S\omega^*$ are the same sign, the term $S\omega^*$ (which is the term isolated by the fitting technique) is less than the total heating by atmospheric dynamics. Similar reasoning applies to regions of anomalous rising motion.

The results of the fitting procedure are shown in Figs. 3c, 3d and 7. Column ozone and T_4 are high correlated on month-to-month timescales at all latitudes (Fig. 5, top), but are not strongly correlated on secular timescales, as evidenced by the different meridional structures in the lower panels in Fig. 5. Consequently, the temperature trends linearly congruent with O_3 (Fig. 7 middle) overpredict the observed temperature trends poleward

of ~50 degrees latitude and underpredict the observed temperature trends equatorward of ~50 degrees latitude. The ozone-residual temperature field is marked by warming over the past few decades in the SH polar regions (and to a lesser extent the NH polar regions) but cooling at tropical, subtropical and middle latitudes equatorward of 50 degrees (Fig. 3d; Fig. 7 bottom)

Why do the trends in column ozone overestimate the observed trends in T_4 at polar latitudes but underestimate the trends in T_4 equatorward of 50 degrees? Ozone is known to have a substantial radiative impact on stratospheric temperatures (e.g., Shine et al. 2003; Chipperfield et al. 2007). Hence the linear relationship between temperature and ozone revealed in Fig. 5 (top) and used to derive the fits in equation (2) should hold not only on month-to-month but also secular timescales. Additionally, most of the variability in column ozone is derived from fluctuations in ozone within the region sampled by the T_4 instrument (Fig. 1a), hence the trends in column ozone should be dominated by trends above the tropopause. The most obvious physical explanation for the pattern of ozone-residual temperature trends in Fig. 7 (bottom) is that the radiative cooling due to ozone depletion is being attenuated by anomalous sinking motion in the polar regions, and is being enhanced by anomalous rising motion in the tropics, subtropics and even middle latitudes of both hemispheres.

5. Discussion

Previous analyses have demonstrated the key role of ozone in driving long-term trends in stratospheric temperatures. However, such studies have not fully examined the

role of ozone in driving the peculiar time history of global-mean stratospheric temperatures. This is because existing attribution studies are based on either profile measurements which do not sample the period immediately following volcanic eruptions (e.g., Shine et al. 2003; Ramawamy et al. 2006) or simulated values of ozone derived from CCMs (e.g., Dameris et al. 2005).

A key difficulty when examining the observed linkages between ozone and the time history of global-mean stratospheric temperatures is the sparse nature of ozone profile measurements. Here we worked around the sparse nature of profile measurements by exploiting the substantial overlap between the MSU4 weighting function and the region of the atmosphere which contributes most to global-mean fluctuations in column ozone. The overlap suggests comparatively well-sampled column ozone measurements can be used as a proxy for ozone in the region sampled by the MSU4 instrument, and hence that column measurements can be used to draw inferences about the contribution of ozone to the time history of T_4 .

The resulting analyses reveal that the distinct drops in global-mean stratospheric temperatures following the transient warming due to the eruptions of El Chichon and Mt. Pinatubo are linearly consistent with concurrent drops in ozone. We note that the several-year period after the eruption of Mt. Pinatubo is unique in the global ozone record, insofar as it is the only period in which concurrent ozone decreases are observed across not only the tropics and NH midlatitudes, but also SH midlatitudes. The analyses further suggest that the weak rise in global-mean temperatures between the eruption of El Chichon and Mt. Pinatubo is consistent with the concomitant weak rise in ozone, and the results clarify that the seemingly mysterious rise in global-mean stratospheric

temperatures since ~1993 is consistent with increasing stratospheric ozone juxtaposed on global-mean cooling of ~0.1 K/decade. Hence, while the solar cycle and variability in upwelling longwave radiation play a role in the time history of global-mean temperatures in recent simulations (e.g., Dameris et al. 2005; Ramaswamy et al. 2006), our analyses suggests that neither factor is necessary to explain the step-like variability that dominates the observed record of T_4 . We argue that the pattern of rising and lowering temperatures following the eruptions of El Chichon and Mt. Pinatubo is consistent with the competing radiative and chemical effects of volcanic eruptions on stratospheric climate.

When the analyses are extended to individual latitude bands, the results suggest that anomalous sinking motion is attenuating ozone-induced cooling at polar latitudes while anomalous rising motion is enhancing stratospheric cooling at tropical, subtropical and middle latitudes. The implied trends towards increased upwelling equatorward of 50 degrees but downwelling in the polar stratosphere are consistent with increased wave driving in the polar stratosphere, as found in numerous recent climate change experiments (Rind et al. 1998; Butchart and Scaife 2001; Eichelberger and Hartmann 2005; Li et al. 2008). To-date, observations of trends in the stratospheric overturning circulation have relied on either 1) derived quantities such as eddy fluxes from reanalyses data (Hu and Tung 2002), which are not viewed as reliable for trend estimates (CCSP 2006), or 2) changes in tropical upwelling inferred from chemical data since 2001 (Randel et al. 2006). The results shown here thus provide additional observational support for changes in the stratospheric overturning circulation based exclusively on observations from the carefully calibrated and relatively long records available from the MSU4 and TOMS instruments.

References

- Bhartia, P.K., J. Herman, R. D. McPeters, and O. Torres, 1993: Effect of Mount Pinatubo Aerosols on Total Ozone Measurements from Backscatter Ultraviolet (BUV) experiments. *J. Geophys. Res.*, **98**, 18547-18554.
- Bodeker, G. E., H. Garny, D. Smale, M. Dameris, and R. Deckert, 2007: The 1985 Southern Hemisphere mid-latitude total column ozone anomaly. *Atmos. Chem. Phys.*, **7**, 5625-5637.
- Butchart, N., and A. A. Scaife, 2001: Removal of chlorofluorocarbons by increased mass exchange between the stratosphere and the troposphere in a changing climate. *Nature*, **410**, 799-802.
- CCSP, 2006: Temperature Trends in the Lower Atmosphere: Steps for Understanding and Reconciling Differences T. R. Karl et al., eds, 164 pp.
- Chipperfield, M. P., et al., 2007: in World Meteorological Organization, 2007: Scientific assessment of ozone depletion: 2006: Global Ozone Research and Monitoring Project Rep. #50, Geneva, Switzerland, 572 pp.
- Dameris, M., et al., 2005: Long-term changes and variability in a transient simulation with a chemistry-climate model employing realistic forcing. *Atmos. Chem. Phys.*, **5**, 2121 – 2145.
- Eichelberger, S.J., and D.L. Hartmann, 2005: Changes in the strength of the Brewer-Dobson circulation in a simple AGCM. *Geophys. Res. Lett.*, **32**, L15807, doi:-10.1029/2005GL022924.
- Eyring, V., 2006: Assessment of temperature, trace species and ozone in chemistry-

- climate model simulations of the recent past, *J. Geophys. Res.*, **111**, D22308, doi:10.1029/2006JD007327.
- Fioletov, V.E., G.E., Bodeker, A.J. Miller, R.D. McPeters, and R. Stolarski, 2002: Global and zonal total ozone variations estimated from ground-based and satellite measurements: 1964-2000. *J. Geophys. Res.*, **107**, doi: 10.1029/2001JD001350.
- Fleming, E. L., C. H. Jackman, D. K. Weisenstein, and M. K. W. Ko, 2007: The impact of interannual variability on multidecadal total ozone simulations. *J. Geophys. Res.*, **112**, D10310, DOI:10.1029/2006JD007953
- Forster, P. M., G. Bodeker, R. Schofield, S. Solomon, and D. W. J. Thompson, 2007: Effects of ozone cooling in the tropical lower stratosphere and upper troposphere. *Geophys. Res. Lett.*, **34**, L23813, doi:10.1029/2007GL031994.
- Gleason, J.F., et al, 1993: Record low global ozone in 1992. *Science*, **260**, 523-526.
- Hu, Y. and K.K. Tung; 2002: Interannual and Decadal Variations of Planetary - Wave Activity, Stratospheric Cooling, and Northern-Hemisphere Annular Mode. *J. Climate*, **15**, 1659-1673.
- Langematz, U., M. Kunze, K. Krüger, K. Labitzke, and G.L. Roff, 2003: Thermal and dynamical changes of the stratosphere since 1979 and their link to ozone and CO₂ changes. *J. Geophys. Res.*, **108**, doi: 10.1029/2002JD002069.
- Li, F., J. Austin, and J. Wilson, 2008: The Strength of the Brewer–Dobson Circulation in a Changing Climate: Coupled Chemistry–Climate Model Simulations. *J. Climate*, **21**, 40-57.
- McCormick, M.P., J.M. Zawodny, R.E. Viega, J.C. Larson and P.H. Wang, 1989: An overview of SAGE I and II ozone measurements. *Planet. Sp. Sci.*, **37**, 1567-1586.

- Mears, C.A., M.C. Schabel, and F.J. Wentz, 2003: A reanalysis of the MSU Channel 2 tropospheric temperature record. *J. Climate*, **16**, 3650-3664.
- Pawson, S., K. Labitzke, and S. Leder, 1998: Stepwise changes in stratospheric temperature. *Geophys. Res. Lett.*, **25**, 2157-2160
- Prather, M., 1992: Catastrophic loss of stratospheric ozone in dense volcanic clouds. *J. Geophys. Res.*, **97**, 10187-10191.
- Ramaswamy, V. et al., 2001: Stratospheric temperature trends: Observations and model simulations. *Rev. Geophys.*, **39**, 71–122.
- Ramaswamy, V., and M. D. Schwarzkopf, 2002: Effects of ozone and well-mixed gases on annual-mean stratospheric temperature trends. *Geophys. Res. Lett.*, **29**, 2064, doi : 10. 1029/2002GL015141.
- Ramaswamy, V., M. D. Schwarzkopf, W. J. Randel, B. D. Santer, B. J. Soden, and G. Stenchikov, 2006: Anthropogenic and natural influences in the evolution of lower stratospheric cooling. *Science*, **311**, 1138 – 1141.
- Randel, W.J., and J.B. Cobb, 1994: Coherent variations of monthly mean total ozone and lower stratospheric temperature. *J. Geophys. Res.*, **99**, 5433-5447.
- Randel, W. J., and F. Wu, 1999: A stratospheric ozone trends data set for global modeling studies. *Geophys. Res. Lett.*, **26**, 3089–3092.
- Randel, W.J, and F. Wu, 2006: Biases in stratospheric and tropospheric temperature trends derived from historical radiosonde data. *J. Climate*, **19**, 2094-2104.
- Randel, W.J., F. Wu, G. Nedoluha, H. Vomel and P. Forster, 2006: Decreases in stratospheric water vapor since 2001: Links to changes in the tropical tropopause and the Brewer-Dobson circulation. *J. Geophys. Res.*, **111**, D12312,

doi:10.1029/2005JD006744.

- Randel, W. J., and F. Wu, 2007: A stratospheric ozone profile data set for 1979–2005: Variability, trends, and comparisons with column ozone data. *J. Geophys. Res.*, **112**, D06313, doi:10.1029/2006JD007339.
- Randel, W. J. et al., 2008: An updated analysis of stratospheric temperature trends. *In preparation*.
- Rind, D., D. Shindell, P. Lonergan, and N.K. Balachandran, 1998: Climate change and the middle atmosphere. Part III: The doubled CO₂ climate revisited. *J. Climate*, **11**, 876-894.
- Robock, Alan, 2000: Volcanic eruptions and climate. *Rev. Geophys.*, **38**, 191-219.
- Rosier, S. M., and K. P. Shine, 2000: The effect of two decades of ozone change on stratospheric temperature, as indicated by a general circulation model. *Geophys. Res. Lett.*, **27**, 2617 – 2620.
- Santer, B. D., T. M. L. Wigley, J. S. Boyle, D. J. Gaffen, J. J. Hnilo, D. Nychka, D. E. Parker, and K. E. Taylor, 2000: Statistical significance of trend differences in layer-average temperature time series. *J. Geophys. Res.*, **105**, 7337–7356.
- Seidel, D.J., and J.R. Lanzante, 2004: An assessment of three alternatives to linear trends for characterizing global atmospheric temperature changes. *J. Geophys. Res.*, **109**, D14108, doi: 10.1029/2003-JD004414.
- Shine, K. P., et al., 2003: A comparison of model-simulated trends in stratospheric temperatures. *Q. J. R. Meteorol. Soc.*, **129**, 1565 – 1588.
- Solomon, S., R. W. Portmann, R. R. Garcia, L. W. Thomason, L. R. Poole, and M. P. McCormick, 1996: The role of aerosol variations in anthropogenic ozone

- depletion at northern midlatitudes. *J. Geophys. Res.*, **101**, 6713-6727.
- Steinbrecht, W., Hassler, B., Claude, H., Winkler, P., and Stolarski, R. S., 2003: Global distribution of total ozone and lower stratospheric temperature variations. *Atmos. Chem. Phys.*, **3**, 1421–1438.
- Stolarski, R. S., A. R. Douglass, S. Steenrod, and S. Pawson, 2006: Trends in stratospheric ozone: Lessons learned from a 3D chemical transport model. *J. Atmos. Sci.*, **63**, 1028 – 1041.
- Thompson, D. W. J., and S. Solomon, 2005: Recent stratospheric climate trends: Global structure and tropospheric linkages. *J. Climate*, **18**, 4785–4795.
- Wang, H. J., D. M. Cunnold, L. W. Thomason, J. M. Zawodny, and G. E. Bodeker, 2002: Assessment of SAGE version 6.1 ozone data quality. *J. Geophys. Res.*, **107**(D23), 4691, doi:10.1029/2002JD002418.
- Yulaeva, E., J.R. Holton and J.M. Wallace, 1994: On the cause of the annual cycle in tropical lower stratosphere temperatures. *J. Atmos. Sci.*, **51**, 169-174.

Figure 1: *Panel (a)* Solid: Weighting function for RSS MSU 4 temperature data (T_4). Dashed: global-mean, monthly-mean ozone anomalies from the SAGE data regressed as a function of altitude onto standardized values of global-mean, monthly-mean total column ozone anomalies from the TOMS/SBUV data. The SAGE data were converted to DU/km before the regression coefficients were calculated. The curves have been normalized so that the area under both curves is equal to one. *Panel (b)* Detrended global-mean, monthly-mean T_4 anomalies vs. detrended global-mean, monthly-mean TOMS/SBUV column ozone anomalies for all months 1979-2006 except the 3 years following the El Chichon and Mt. Pinatubo eruption dates. *Panel (c)* Time series of global-mean, monthly-mean T_4 anomalies (black) and global-mean, monthly-mean TOMS/SBUV column ozone anomalies (red). The vertical dashed lines denote the El Chichon and Mt. Pinatubo eruption dates.

Figure 2. (top) Time series of global-mean, monthly-mean T_4 anomalies reproduced from Fig. 1c; (middle) the component of the global-mean T_4 time series that is linearly congruent with the time series of global-mean, monthly-mean TOMS/SBUV column ozone anomalies from Fig. 1c; (bottom) the ozone-residual T_4 time series. The fitting procedure and trend calculations are described in the text. The vertical dashed lines denote the El Chichon and Mt. Pinatubo eruption dates.

Figure 3. *Panels a) and b):* Zonal-mean, monthly-mean time series of (a) TOMS/SBUV column ozone anomalies and (b) T_4 anomalies. The horizontal dashed line denotes the Mt. Pinatubo eruption date. Contour plots are smoothed with a 5 month running mean

filter for display purposes only. Note the data are in anomaly form and hence do not exhibit a seasonal cycle. *Panels c) and d)*: As in panels a) and b) but for (c) the components of the zonal-mean, monthly-mean T_4 anomaly time series that are linearly congruent with the TOMS/SBUV column ozone anomaly time series; and (d) the associated ozone-residual T_4 anomaly data. Note the fitted and residual time series are found as a function of latitude band and are given by Eq. 2.

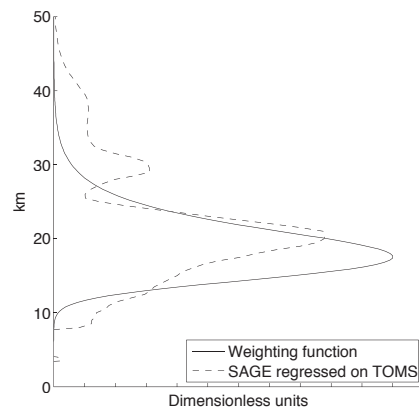
Figure 4. Time series of monthly-mean TOMS/SBUV column ozone anomalies for latitude bands indicated. The vertical dashed lines denote the El Chichon and Mt. Pinatubo eruption dates and the horizontal lines represent the means for the period 1986-1990.

Figure 5. (top) Correlations between the zonal-mean, monthly-mean T_4 and TOMS/SBUV column ozone anomaly data as a function of latitude. The correlations are calculated for all months 1979-2006 except the 3 years following the El Chichon and Mt. Pinatubo eruption dates. The horizontal dashed line denotes the 1-tailed 95% confidence level assuming 1 degree of freedom per year. (middle) Linear trends in T_4 and (bottom) TOMS/SBUV column ozone as a function of latitude. Error bars denote the 95% significance level of the trends.

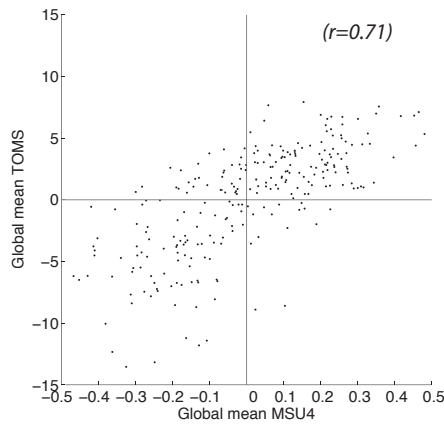
Figure 6. Time series of zonal-mean, monthly-mean TOMS/SBUV column ozone and T_4 anomalies for latitude bands indicated. Values of zero denote the long-term mean.

Figure 7. (top) Linear trends in T_4 reproduced from Fig. 5; (middle) the component of the trends linearly congruent with variability in zonal-mean, monthly-mean TOMS/SBUV column ozone anomalies; (bottom) the ozone-residual temperature trends. The gray lines in the middle and bottom panels denote results based on ground-based Dobson data. See text for details of the fitting procedure.

a) T4 weighting function and SAGE regressed on TOMS/SBUV



b) Scatter plot of global mean T4 and TOMS/SBUV



c) Global mean T4 and TOMS/SBUV ozone

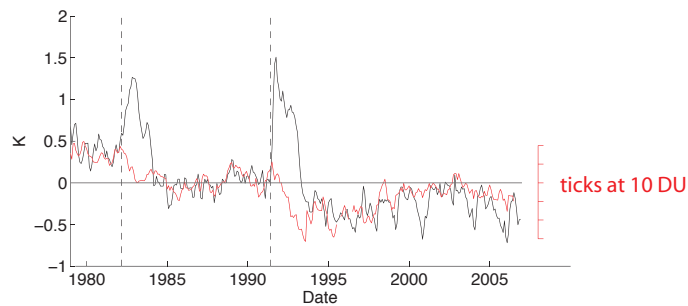


Figure 1: Panel (a) Solid: Weighting function for RSS MSU 4 temperature data (T4). Dashed: global-mean, monthly-mean ozone anomalies from the SAGE data regressed as a function of altitude onto standardized values of global-mean, monthly-mean total column ozone anomalies from the TOMS/SBUV data. The SAGE data were converted to DU/km before the regression coefficients were calculated. The curves have been normalized so that the area under both curves is equal to one. Panel (b) Detrended global-mean, monthly-mean T4 anomalies vs. detrended global-mean, monthly-mean TOMS/SBUV column ozone anomalies for all months 1979-2006 except the 3 years following the El Chichon and Mt. Pinatubo eruption dates. Panel (c) Time series of global-mean, monthly-mean T4 anomalies (black) and global-mean, monthly-mean TOMS/SBUV column ozone anomalies (red). The vertical dashed lines denote the El Chichon and Mt. Pinatubo eruption dates.

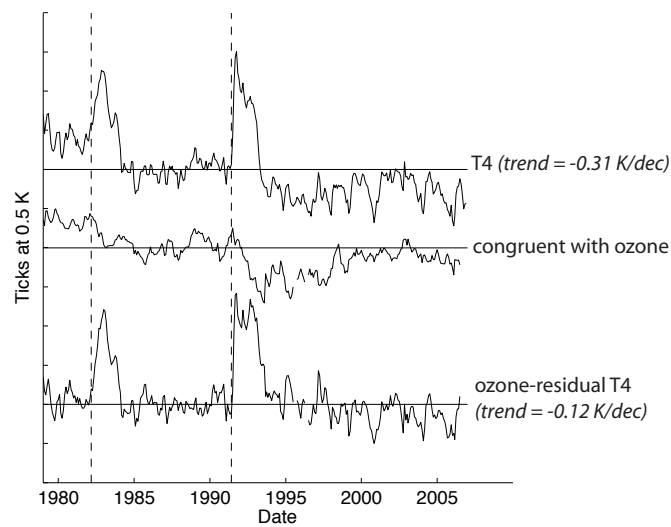


Figure 2. (top) Time series of global-mean, monthly-mean T4 anomalies reproduced from Fig. 1c; (middle) the component of the global-mean T4 time series that is linearly congruent with the time series of global-mean, monthly-mean TOMS/SBUV column ozone anomalies from Fig. 1c; (bottom) the ozone-residual T4 time series. The fitting procedure and trend calculations are described in the text. The vertical dashed lines denote the El Chichon and Mt. Pinatubo eruption dates.

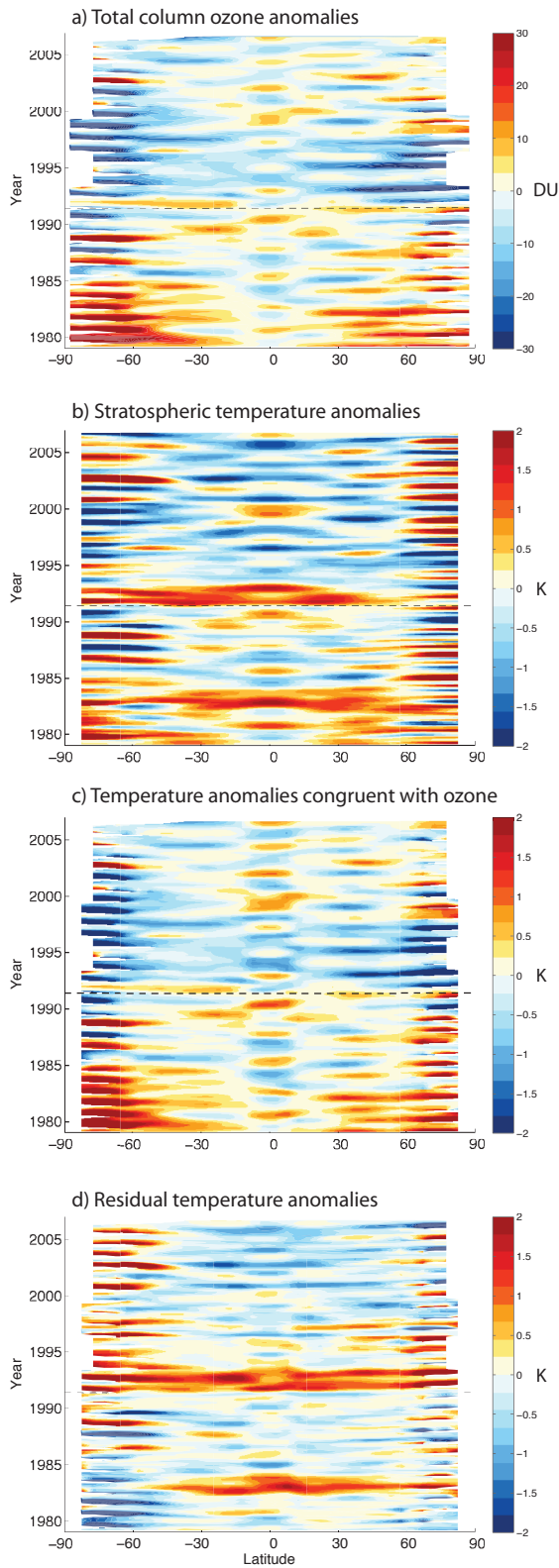


Figure 3. Panels a) and b): Zonal-mean, monthly-mean time series of (a) TOMS/SBUV column ozone anomalies and (b) T4 anomalies. The horizontal dashed line denotes the Mt. Pinatubo eruption date. Contour plots are smoothed with a 5 month running mean filter for display purposes only. Note the data are in anomaly form and hence do not exhibit a seasonal cycle. Panels c) and d): As in panels a) and b) but for (c) the components of the zonal-mean, monthly-mean T4 anomaly time series that are linearly congruent with the TOMS/SBUV column ozone anomaly time series; and (d) the associated ozone-residual T4 anomaly data. Note the fitted and residual time series are found as a function of latitude band and are given by Eq. 2.

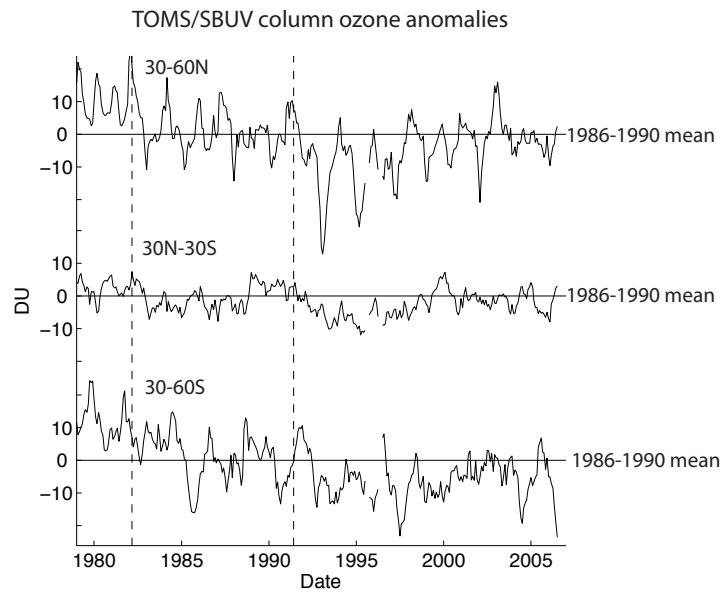


Figure 4. Time series of monthly-mean TOMS/SBUV column ozone anomalies for latitude bands indicated. The vertical dashed lines denote the El Chichon and Mt. Pinatubo eruption dates and the horizontal lines represent the means for the period 1986-1990.

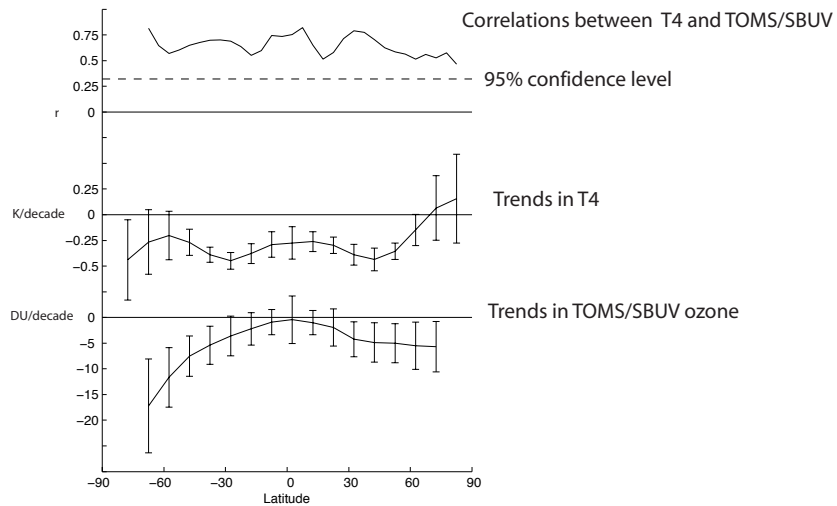


Figure 5. (top) Correlations between the zonal-mean, monthly-mean T4 and TOMS/SBUV column ozone anomaly data as a function of latitude. The correlations are calculated for all months 1979-2006 except the 3 years following the El Chichon and Mt. Pinatubo eruption dates. The horizontal dashed line denotes the 1-tailed 95% confidence level assuming 1 degree of freedom per year. (middle) Linear trends in T4 and (bottom) TOMS/SBUV column ozone as a function of latitude. Error bars denote the 95% significance level of the trends.

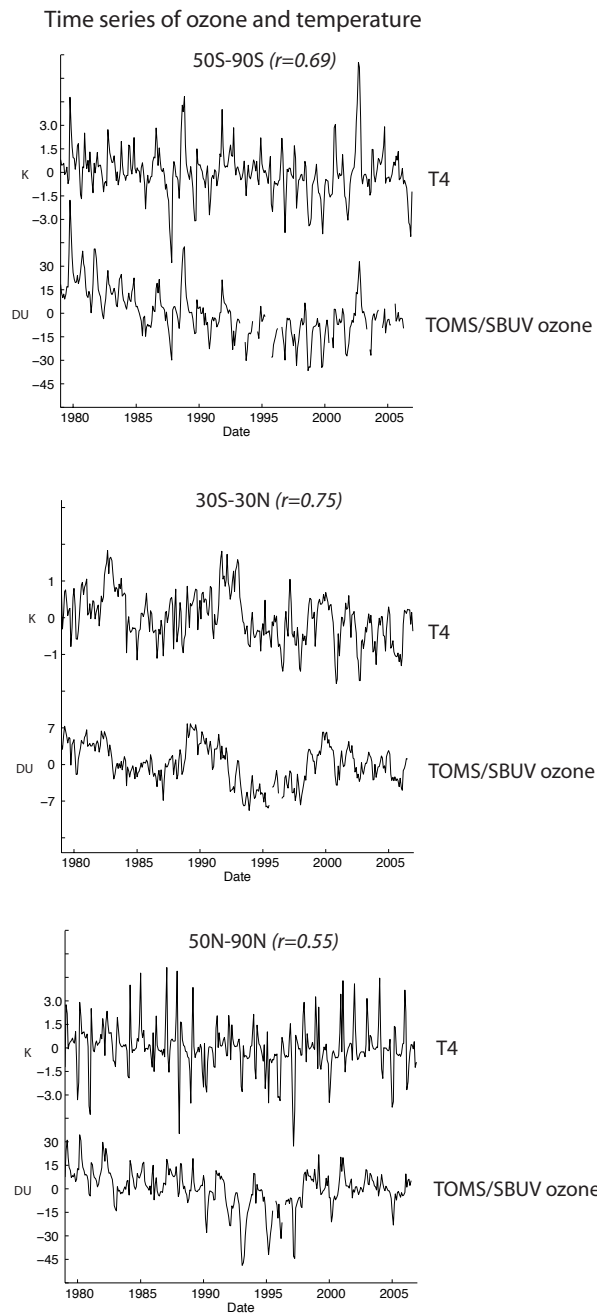


Figure 6. Time series of zonal-mean, monthly-mean TOMS/SBUV column ozone and T4 anomalies for latitude bands indicated. Values of zero denote the long-term mean.

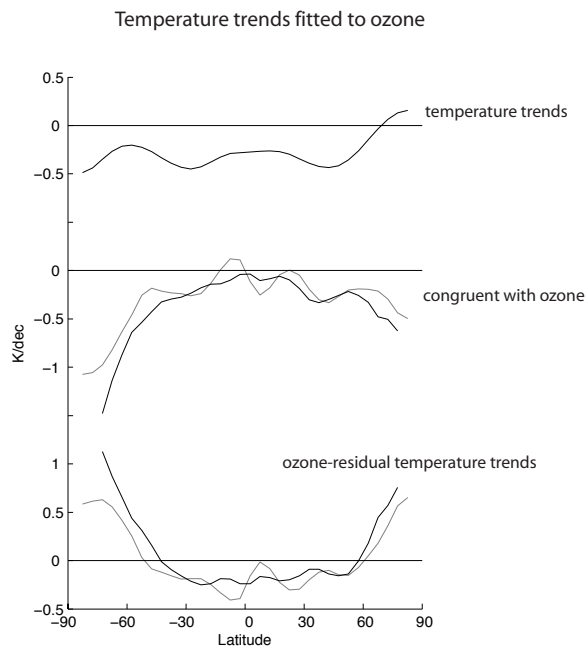


Figure 7. (top) Linear trends in T4 reproduced from Fig. 5; (middle) the component of the trends linearly congruent with variability in zonal-mean, monthly-mean TOMS/SBUV column ozone anomalies; (bottom) the ozone-residual temperature trends. The gray lines in the middle and bottom panels denote results based on ground-based Dobson data. See text for details of the fitting procedure.